

SUPERCONDUCTING PROTOTYPE CAVITIES FOR THE SPALLATION NEUTRON SOURCE (SNS) PROJECT *

G. Ciovati, P. Kneisel[†], J. Brawley, R. Bundy, I. Campisi, K. Davis, K. Macha, D. Machie, J. Mammosser, S. Morgan, R. Sundelin, L. Turlington, K. Wilson, Jefferson Lab; M. Doleans, S.H. Kim, D. Mangra, ORNL-SNS; D. Barni, C. Pagani, P. Pierini, INFN Milano; K. Matsumoto, R. Mitchell, D. Schrage, LANL; R. Parodi, INFN Genova; J. Sekutowicz, DESY; P. Ylae-Oijala, Univ. Helsinki

Abstract

The Spallation Neutron Source project includes a superconducting linac section in the energy range from 186 MeV to 1000 MeV. For this energy range two types of cavities are needed with geometrical β values of $\beta=0.61$ and $\beta=0.81$. An aggressive cavity prototyping program is being pursued at Jefferson Lab, which calls for fabricating and testing four $\beta=0.61$ cavities and two $\beta=0.81$ cavities. Both types consist of six cells made from high purity niobium and feature one HOM coupler on each beam pipe and a port for a high power coaxial input coupler. Three of the four $\beta=0.61$ cavities will be used for a cryomodule test in early 2002. At this time four medium beta cavities and one high beta cavity have been completed at JLab. The first tests on the $\beta=0.61$ and $\beta=0.81$ exceeded the design values for gradient and Q value: $E_{acc} = 10.1$ MV/m and $Q = 5 \times 10^9$ at 2.1K for the $\beta=0.61$ and $E_{acc} = 12.3$ MV/m and $Q = 5 \times 10^9$ at 2.1 K for the $\beta=0.81$. One of the medium beta cavities has been equipped with an integrated helium vessel and measurements of the static Lorentz force detuning have been done and compared to the "bare" cavities.

In addition two single cell cavities have been fabricated, equipped with welded-on HOM couplers. They are being used to evaluate the HOM couplers with respect to multipacting, fundamental mode rejection and HOM damping as far as possible in a single cell.

This paper describes the cavity design with respect to electromagnetic and mechanical features, the fabrication efforts and the results obtained with the different cavities existing at the time of this workshop.

1 ELECTROMAGNETIC DESIGN

The designs for the two types of SNS cavities were dominated by the desire to keep the electric peak surface field at or below 27.5 MV/m and the magnetic peak surface field below 60 mT. At the same time the Lorentz force detuning coefficient (K_L) should not exceed a value of -3 Hz/(MV/m)². By choosing a cell-to-cell coupling of 1.5% for these six-cell cavities a reasonably small ratio of peak surface fields and accelerating fields could be

realized [1], if four different half cell shapes were used. The fundamental power coupler (FPC) requirement for a Q_{ext} value of about 10^6 implied larger iris and equator diameters for the end half cells at the FPC side (see figure 1) compared to the center cells. Simulation calculations done with the center cell geometries and the full cavities showed that multipacting was unlikely because the emitted electrons don't gain enough energy to yield secondary emission. The specifications for the Lorentz coefficient require welded stiffening rings between the cell irises at a radius of 80 mm from the cavity axis. The SNS cavities have Nb55Ti flanges throughout (DESY-type), sealed with AlMg₃ gaskets: one at each tapered beam pipe end, two ports (one for each end) for the HOM couplers, rotated 115 degrees with respect to each other, a port for the field probe and one for the FPC. The coaxial FPC is the KEK design scaled to 805 MHz [2]. Table 1 lists the basic electromagnetic parameters for the SNS cavities. The Lorentz force coefficient (K_L) is for fixed (ideal) boundary conditions.

Table 1: SNS cavities' electromagnetic parameters.

Cavity β	0.61	0.81
Frequency [MHz]	805.000	805.000
E_{peak}/E_{acc}	2.71	2.19
B_{peak}/E_{acc} [mT/(MV/m)]	5.72	4.72
R/Q [Ω]	279	483
$G (=R_s Q_0)$ [Ω]	179	260
Cell-to-cell k [%]	1.53	1.52
K_L [Hz/(MV/m) ²]	-2.07	-0.43

2 FABRICATION

The SNS cavity cells are fabricated from RRR > 250 niobium. The dumbbells exhibited significant mechanical deformations after the attachment of the stiffening rings. This required re-adjustments of mechanical dimensions and frequencies of the dumbbells in a way similar to that described in [3]. The dumbbell had to be stretched and trimmed at the equator to reach both the right length and frequency. Once the dumbbells had been corrected, the electron beam welding of the cavity assembly started from the two end groups by adding dumbbells; the last

* Work supported by the U.S. DOE Contract No DE-AC05-00-OR22725

[†]kneisel@jlab.org

weld was the equator weld of the two half sub-assemblies.

Tuning to a "flat" field profile followed after a 20 μm external chemistry. Internal buffered chemical polishing (BCP) in JLab's closed chemistry system with $\sim 120 \mu\text{m}$ material removal and subsequent high pressure ultrapure water rinsing for 2 h completed the final surface treatment. After drying for several hours the cavity was assembled in the class 100 clean room.

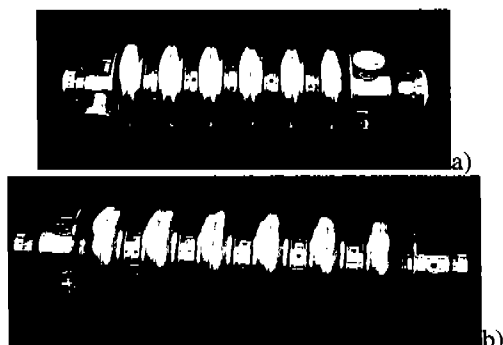


Figure 1: SNS $\beta=0.61$ (a) and $\beta=0.81$ (b) prototype cavities.

In July the three medium beta cavities needed for the prototype cryomodule were completed (figure 2). The frequency of the "as fabricated" was within 150 kHz of the target value and the field-flatness was about 30%.

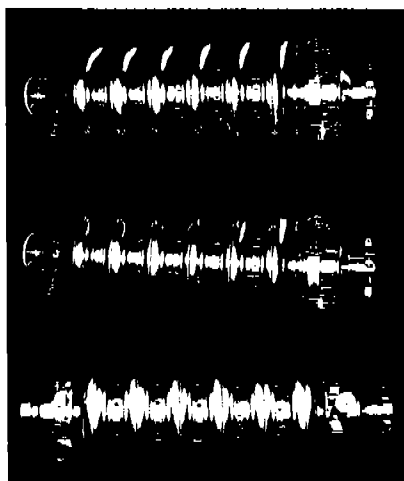


Figure 2: SNS $\beta=0.61$ cavities for the prototype cryomodule.

The prototype titanium helium vessel has been TIG welded on the first of the four medium beta prototype cavities (figure 3), this cavity won't be used for the prototype cryomodule. The frequency decreased by about 300 kHz due to the weld shrinkage and the field profile tilted by about 15%. These changes are of some concern for the prototype cryomodule cavity string and need to be understood and minimized.

The cavity with He vessel has been processed with BCP for 15 min. and high pressure rinsed for about 2 h. Results are discussed in section 3.

The He vessel that will be used for production cavities will be stiffened by welding titanium cones on the two heads [4] to lower the Lorentz force coefficient.

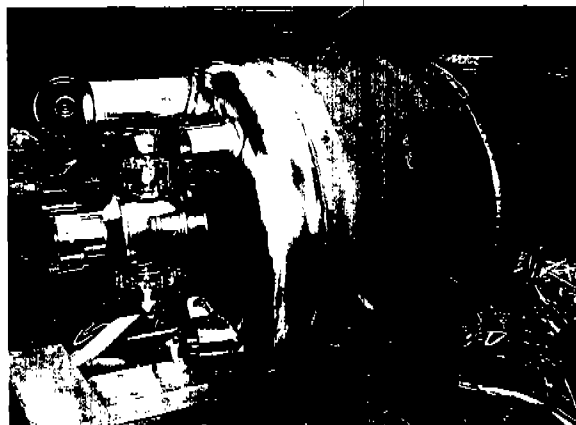


Figure 4: titanium He vessel welded on the $\beta=0.61$ prototype cavity.

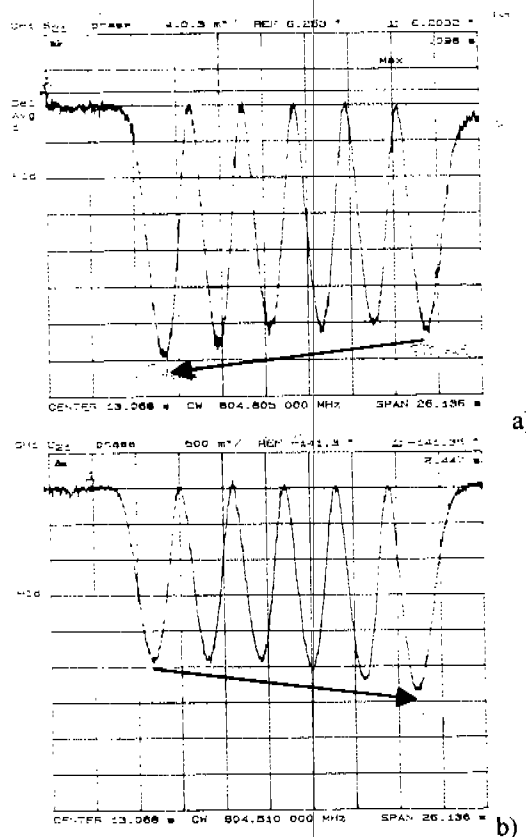


Figure 5: stored energy in each cell of the cavity before (a) and after (b) welding the He vessel.

3 VERTICAL TEST RESULTS

The results of the vertical test for the six-cells $\beta=0.61$ prototype cavity before and after the welding of the He vessel are shown in figure 6. The "bare" cavity had a Q_0 at low field of about 2.3×10^{10} . No multipacting barrier has been found and, after about 20 min of RF processing, the

cavity reached $E_{acc}=16$ MV/m with a Q of 1.4×10^{10} , exceeding comfortably the design goal for this cavity type. After welding the He vessel, the cavity has been tested at 2.1K. The Q at low field was 1.3×10^{10} and field emission started at about 6 MV/m, lowering the Q to 2.9×10^9 at 10.1 MV/m. We believe that the degradation of performance after the addition of He vessel is due to insufficient surface chemistry.

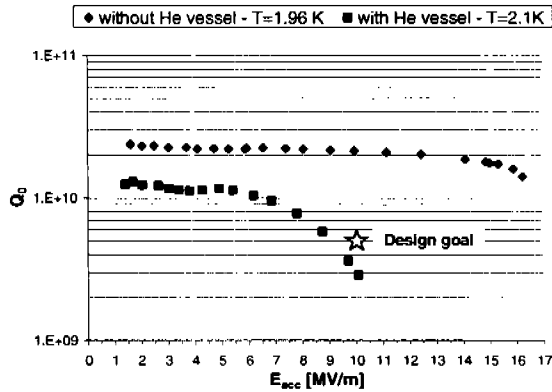


Figure 6: SNS $\beta=0.61$ vertical test results.

The results for the six-cells $\beta=0.81$ prototype cavity at three different temperatures are shown in figure 7. The Q_0 at low field was about 2.9×10^{10} . From the temperature dependence of the surface resistance a residual resistance of 7.9 n Ω was extracted. Also this cavity did not show any multipacting as predicted, but field emission started at about $E_{acc}=13$ MV/m. After about 20 min of He processing the cavity reached $E_{acc}=19$ MV/m with a Q of 8.3×10^9 .

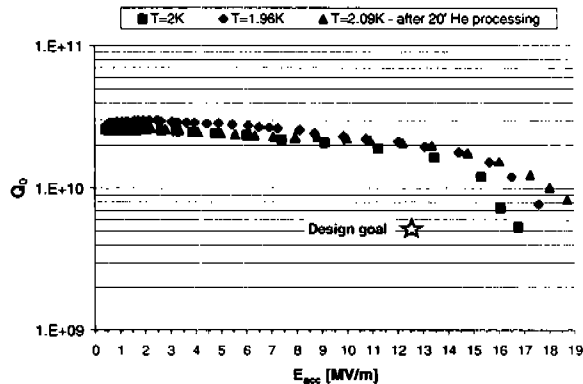


Figure 7: SNS $\beta=0.81$ vertical test results.

4 MECHANICAL ANALYSIS

4.1 Lorentz force detuning

During the cryogenic tests the static Lorentz force coefficient was also measured for three different boundary conditions for the $\beta=0.61$ cavity: a titanium frame used to support the bare cavity, the He vessel and He vessel plus a mock-up tuner, shown in figure 8. This data were used to

validate the 3D model of the cavity that should predict the Lorentz coefficient for the production assembly configuration of cavity-He vessel-tuner. SUPERFISH was used to compute radiation pressures on the walls of the cavities and the resonant frequencies. With the finite element code ABAQUS the shape deformations due to the Lorentz pressure, with different boundary conditions, were calculated for an accurate model of the SNS cavities. The results from the calculations are in good agreement (15%) with the experimental data (table 2). The highest value is for the cavity with the He vessel only, because of the low spring constant of the bellow (about 250 kg/cm).

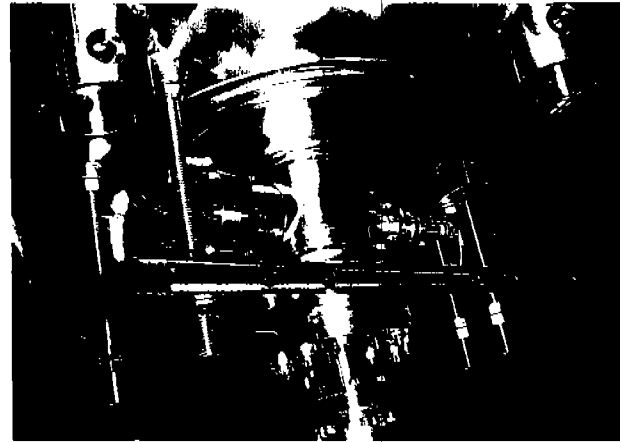


Figure 8: Mock-up tuner bolted onto the He vessel.

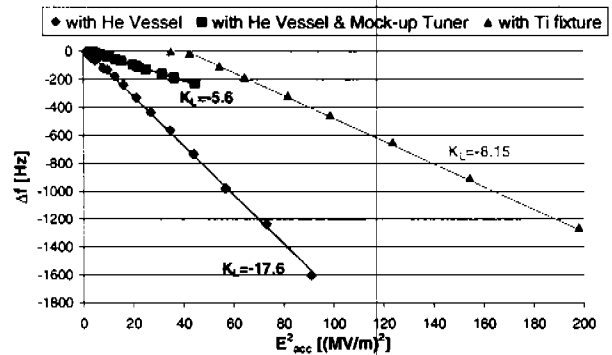


Figure 9: SNS $\beta=0.61$ frequency shift vs. E_{acc}^2 measured for three different boundary conditions.

Table 2: Lorentz coefficient K_L [Hz/(MV/m)²] measured and computed with different boundary conditions.

Cavity β	0.61		0.81	
	Measured	Model	Measured	Model
Fixed end	-	-1.65	-	-0.43
Mock-up tuner	-5.6	-5.2	-	-
Ti frame	-7.85	-7.0	-3.62	-3.5
He vessel	-18	-21	-	-

The calculations for the production assembly cavity-He vessel-tuner resulted in a static Lorentz force coefficient of about -3.64 Hz/(MV/m)² for the medium beta cavity (above the specifications), while it is within the

specifications for the high beta. The effects of the 60 Hz RF pulses on the Lorentz force coefficient have been analysed in ref [4].

4.2 Natural Frequencies and Microphonics

A natural frequency vibration test was performed on the prototype medium and high beta niobium cavity, supported with nylon straps at the ends of the beam tubes. A shaker was fixed onto the equator of one of the center cells (figure 10) and a tri-axial accelerometer was attached to an adjacent cell. An additional axial accelerometer was mounted to the FPC-end flange. (See figure 10)



Figure 10: $\beta=0.61$ natural frequency vibration test set-up.

ABAQUS was used again to model the natural frequency spectrum of the cavity; the computed frequencies are in close agreement with the test results as listed in table 3 and 4. To help provide insight into the natural frequencies of the cavity within the cryomodule assembly, the ABAQUS cavity model will be extended to include cryomodule components [5]. The test on the $\beta=0.81$ cavity has been done after the stiffening rings had been cut.

Table 3: Comparison of test data and finite element analysis for the $\beta=0.61$ cavity.

Mode	Natural frequencies [Hz]	
	Test data	FE Analysis
1	13	14
2	31	26
3	38	40
4	53	48
5	70	72
6	82	83
7	125	124

Table 4: Comparison of test data and finite element analysis for the $\beta=0.81$ cavity.

Mode	Natural frequencies [Hz]		
	Test data w/out stiffeners	Model w/out stiffeners	Model with stiffeners
1	11	11	15
2	24	19	29
3	34	38	46
4	45	46	55
5	59	55	83
6	76	74	92
7	103	103	152

A measure of the frequency shift due to microphonics was done on the $\beta=0.61$ cavity integrated in the He vessel before and after attaching the mock-up tuner. The test was done with the cavity at 2K in the vertical dewar. The frequency variations were detected monitoring the output of the phase-locked loop with a custom instrument [6] connected to a dynamic signal analyser. The source of microphonics was provided by mechanical vibration in the Vertical Test Area. As can be seen in figure 11, the FWHM of the histograms curve is lowered by about a factor of 4 when the mock-up tuner is bolted to the He-vessel.

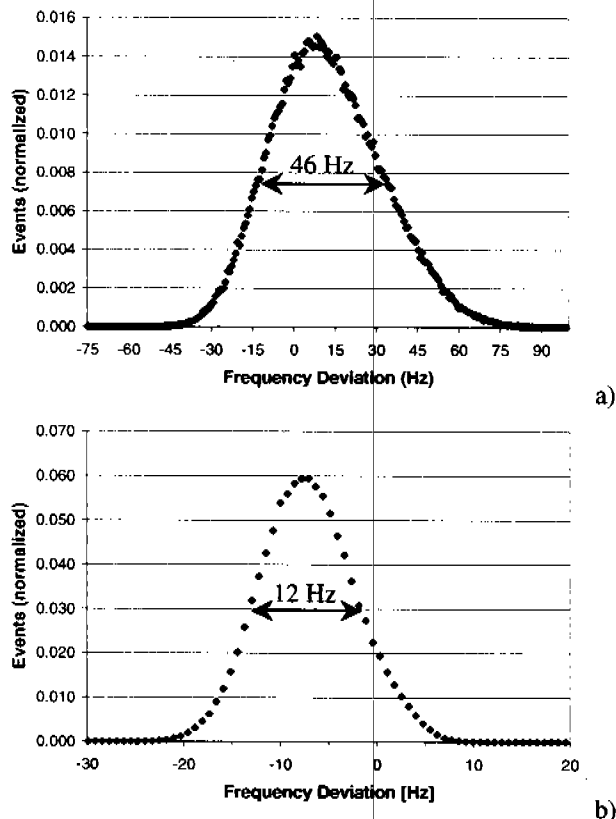


Figure 11: frequency shift due to microphonics measured on the $\beta=0.61$ cavity with he vessel (a) and with mock-up tuner (b).

5 HIGH ORDER MODES ANALYSIS

HOM calculations have been done with MAFIA and SUPERFISH for both types of cavities. Three TM monopole modes for each cavity have frequency close to a bunch harmonic and need adequate damping [7]. These modes have been identified on the copper models and have been damped with high order mode couplers of the DESY-type after optimization of the orientation, as shown in tables 5 and 6. With these values of Q_{ext} , the maximum power dissipated into the cavities due to excitation of an high order mode is limited to 1 W.

Table 5: Measured Q_{ext} and frequencies for the dangerous modes on the $\beta=0.61$ cavity.

Mode	Freq. [MHz]	Q_{ext} @ FPC side	Q_{ext} @ probe side
TM ₀₂₁ -5 π /6 (#31)	2818.79	2×10^5	4×10^4
TM ₀₂₁ - π (#32)	2837.93	2.7×10^5	5×10^5
Beam pipe mode	3221.30	2.5×10^3	-

Table 5: Measured Q_{ext} and frequencies for the dangerous modes on the $\beta=0.81$ cavity.

Mode	Freq. [MHz]	Q_{ext} @ FPC side	Q_{ext} @ probe side
TM ₀₂₁ -5p/6 (#25)	2395.31	1.3×10^4	1.5×10^5
TM ₀₁₂ -p/6 (#35)	2790.87	1.6×10^5	1.4×10^4
Hybrid (#36)	2805.83	2.3×10^4	1.1×10^4

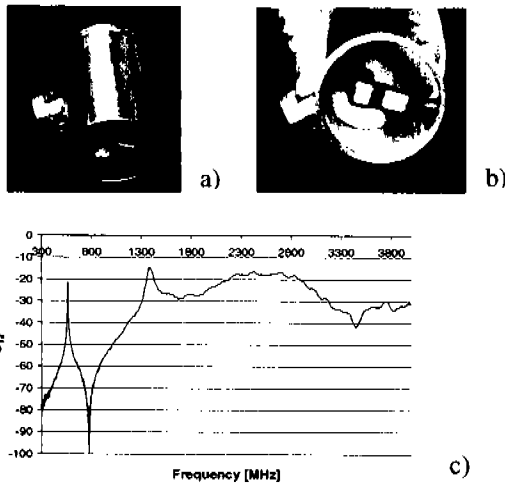


Figure 12: HOM filter (a), (b) and filter characteristic (c).

A single cell $\beta=0.61$ with HOM couplers has been tested in order to verify the absence of multipacting or excessive heating into the couplers. The cavity itself was not tested without HOM filters.

The performance of the cavity is shown in figure 13: field emission started at about $E_{acc}=6$ MV/m and after about 1 h of RF processing the accelerating field went up to 12.4 MV/m with a Q of 5.3×10^9 . No evidence of multipacting or excessive heating from the HOM coupler was detected.

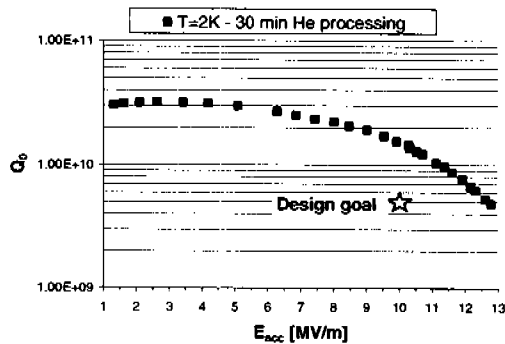


Figure 13: Q vs. E_{acc} for the single cell $\beta=0.61$ with HOM couplers

A single cell $\beta=0.81$ with the FPC-end cell geometry with HOM couplers has also been fabricated to check potential heating problems due to the higher field at the FPC side of the cavity. No measurements have been done yet on this cavity.

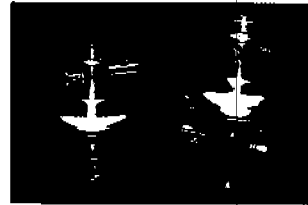


Figure 13: single cells with HOM couplers.

6 SUMMARY

It had been demonstrated that in both types of SNS cavities the design goals for Q -value and accelerating gradient can be achieved with some comfortable margin. Multipacting is no problem and the dangerous higher order modes can be damped appropriately. The mechanical behavior of the cavities has been analyzed; as a result, it appear very difficult to meet the Lorentz force coefficient specification for the medium beta cavity. Another issue is to prevent excessive detuning of the cavities as a result of the addition of the He vessel and and maintain the same performances. The three medium beta cavities needed for the prototype cryomodule are going to be tested in the coming weeks. As a precaution against possible "Q- disease", these cavities will be hydrogen degassed at 800° C.

7 REFERENCES

- [1] P. Pierini et al., "SC Cavity Design for the 700 MHz TRASCO Linac", EPAC '00, Vienna, June 26-30, 2000.
- [2] Y. Kang et al., "Electromagnetic Simulations and Properties of the Fundamental Power Couplers for the SNS Superconducting Cavities", PAC '01, Chicago, June 18-22, 2001.
- [3] G. Kreps, D. Proch and J. Sekutowicz, "Half Cell and Dumbbell Frequency Testing for the Correction of the TESLA Cavity Length", 9th RF Superconductivity Workshop, Santa Fe, Nov. 1-5, 1999, paper WEP031.
- [4] R. Mitchell et al., "Lorentz Force Detuning Analysis of the SNS Accelerating Cavities", these proceedings.
- [5] K. Matsumoto et al., "Vibration Analyses of the SNS Cryomodules", these proceedings.
- [6] G. Davis et al., "Microphonics Testing of the CEBAF Upgrade 7-Cell Cavity", PAC '01, Chicago, June 18-22, 2001.
- [7] S-H. Kim, R. Sundelin, "SNS HOM Damping Requirements via Bunch Tracking", PAC '01, Chicago, June 18-22, 2001.

8 ACKNOWLEDGEMENT

We would like to thank all our colleagues who contributed to this work.